C-Type Inactivation of a Voltage-Gated K^+ Channel Occurs by a Cooperative Mechanism

György Panyi,*‡ ZuFang Sheng,* LiWei Tu,* and Carol Deutsch*
* Department of Physiology, University of Pennsylvania, Philadelphia, Pennsylvania 19104-6085 USA; and ‡ Department of Biophysics, Medical University School of Debrecen, Debrecen, Hungary

ABSTRACT The lymphocyte voltage-gated K^+ channel, Kv1.3, inactivates by a C-type process. We have elucidated the molecular basis for this process using a kinetic analysis of wild-type and mutant (A413V) Kv1.3 homo- and heteromultimeric currents in a mammalian lymphoid expression system. The medians of the measured inactivation time constants for wild-type and A413V homotetrameric currents are 204 and 4 ms, respectively. Co-expression of these subunits produces heteromultimeric channels manifesting inactivation kinetics intermediate between those of wild-type and A413V homomultimers. We have considered several models in which each subunit acts either independently or cooperatively to produce the observed inactivation kinetics. The cooperative model gives excellent fits to the data for any heteromultimeric composition of subunits, clearly distinguishing it from the independent models. In the cooperative model, the difference in free energy between the open and inactivated states of the channel is invariant with subunit composition and equals ~1.5 kcal/mol. Each subunit contributes equally to the activation free energy for transitions between open and inactivated states, with an A413V subunit decreasing the free energy barrier for inactivation (and for recovery from inactivation) by ~0.6 kcal/mol. Our results are consistent with a physical model in which the outer mouth of the channel constricts during C-type inactivation (G. Yellen, D. Sodickson, T. Chen, and M. E. Jurman, 1994, *Biophys. J.* 66:1068–1075).

INTRODUCTION

Two distinct processes underlie the inactivation of voltage-gated K^+ channels during prolonged depolarization. One process, called N-type inactivation, involves a tethered cytoplasmic blocker (inactivation particle) that binds to a receptor site at the inner mouth of the channel (Zagotta et al., 1990; Demo and Yellen, 1991). This binding reaction is inhibited by internally applied tetraethylammonium (TEA) (Choi et al., 1991). Block and unblock of K^+ channels by TEA is fast relative to the inactivation of the channels, competing with an inactivation particle to occlude the pore (Choi et al., 1991). Using a point mutation that removes scorpion toxin sensitivity, together with a mutation that removes inactivation, MacKinnon et al. (1993) showed that the inactivation rate constant for a *Shaker* K^+ channel with one inactivation particle was one-fourth that of a homotetrameric channel with four inactivation particles, whereas the rate of recovery is independent of the subunit composition. Thus, a single inactivation particle is necessary and sufficient for N-type inactivation, and each inactivation particle of a tetrameric channel acts independently (MacKinnon et al., 1993). By contrast, the mechanism of C-type inactivation is unknown. It is usually a slower process, is inhibited by external but not internal TEA (Grissmer and Cahalan, 1989; Choi et al., 1991), and is sensitive to external cations and amino acid composition of the K^+ channel pore (López-Barneo et al., 1993). We show here that all four subunits participate cooperatively in C-type inactivation, a mechanism fundamentally different from the independent contributions by individual subunits in N-type inactivation. These findings support a proposed mechanism whereby the outer mouth of the channel constricts during C-type inactivation (Yellen et al., 1994). Some of these results have been reported in abstract form (Levy et al., 1995).

Received for publication 21 March 1995 and in final form 5 June 1995.

Address reprint requests to Dr. Carol Deutsch, Department of Physiology, University of Pennsylvania, Philadelphia, PA 19104-6085. Tel.: 215-898-8014; Fax: 215-573-5851.

G. P. is visiting from the Department of Biophysics, Medical University School of Debrecen, Debrecen, Nagyerdei, krt. 98, Hungary.

0006-3495/95/09/896/08 $2.00

MATERIALS AND METHODS

CTLL-2 transfection

Cytotoxic murine T cells (CTLL-2) were transiently co-transfected with plasmids encoding the human wild-type (pRc/CMV/WT) or a mutated (pRc/CMV/A413V) Kv1.3 channel along with a Ccd4neo plasmid, containing the gene for human membrane surface CD4, at a molar ratio of 5:1 (32 μg/ml total DNA). For the co-transfection of two K^+ channel genes into CTLL, a double gene plasmid was used containing the mutant K^+ channel insert (CMV/A413V) in a pRc/CMV/CD20 plasmid, which encodes the CD20 membrane surface molecule. This double gene plasmid was co-transfected along with the plasmid containing the WT channel gene (pRc/CMV/WT) at ratios ranging from 1:1 to 1:3.25 (103–210 μg/ml total DNA) using electroporation (Deutsch and Chen, 1993).

CTLL-2 cells were cultured for 24 h in fresh medium before transfection and collected in the logarithmic phase of growth. Cells were suspended in Hanks'-20 mM HEPES balanced salt solution (pH = 7.23) at 2×10^7 cells/ml, and the appropriate mixture of DNA was added to the cell suspension. This suspension was transferred to electroporation cuvettes (400 μl/cuvette, 4 mm electrode gap), kept on ice for 10 min, and then electroporated using a BTX electroporator (San Diego, CA) with settings previously determined to give ~50% viability at 24 h post-transfection (725 V/cm, 2200 μF, 13 Ω). The resultant time constants were 24–25 ms. Cells were incubated for an additional 10 min on ice, transferred back to culture medium (~0.5×10^6 cells/ml), and cultured for 20–28 h at 37°C, 5% CO_2.

Electrophysiology

CTLL-2 cells were collected from culture and incubated with monoclonal mouse anti-human CD4 or CD20 antibody (0.5 $\mu g/10^6$ cells, AMAC, Westbrook, ME) and the $CD4^+$ or $CD20^+$ transfectants were adhered to petri dishes (35 mm) coated with goat anti-mouse IgG as described previously (Matteson and Deutsch, 1984; Deutsch and Chen, 1993). Dishes were washed gently five times with 1 ml normal extracellular bath medium (see below) for the patch-clamp experiments. Standard whole cell patch-clamp techniques were used, as described previously (Matteson and Deutsch, 1984). Pipettes were made from SG10 glass (Richland Glass Co., Richland, NJ), coated with Sylgard 184 (Dow Corning, Midland, MI), and fire-polished to give electrodes of 2–3 MΩ resistance in the bath. The bath solution was (in mM): 140 NaCl, 5 KCl, 1 $MgCl_2$, 2.5 $CaCl_2$, 5.5 glucose, 10 HEPES, and recombinant interleukin-2 (8.3 ng/ml) (pH 7.35, 305 mOsm). The pipette solution was (in mM): 140 KF, 11 K_2EGTA, 1 $CaCl_2$, 2 $MgCl_2$, and 10 HEPES (pH 7.20, 295 mOsm). Because of the large amplitude of K^+ currents in transfected cells, we used up to 70% compensation of the series resistance. Holding potential was between −120 and −130 mV. Current recordings started 2–5 min after achieving the whole cell configuration. In most cases the characteristics of the K^+ current were stable for 12–15 min after starting the recordings; therefore the K^+ current properties reported here were obtained from traces taken ~10 min after whole cell configuration was achieved. All experiments were carried out at room temperature.

Data analysis

Before analysis, current traces were corrected for ohmic leak and for voltage error caused by series resistance (program by D. Levy and G. Panyi). Because both peak conductance and inactivation kinetics of Kv1.3 are voltage-independent at membrane potentials >+20 mV, the corrected current traces for data obtained at +50 mV can be used to determine inactivation time constants. Voltage errors due to series resistance (R_s) were typically ~6 mV. The current traces were corrected assuming that voltage error caused by R_s affects both the leak current (I_{leak}) at holding potential (HP) as well as the membrane current (I_m) at positive test potentials (TP). Series resistance was determined from the position of the access conductance potentiometer on the EPC-7 amplifier. Assuming 0 mV is the reversal potential for the leak current, the leak resistance (R_{leak}) was calculated from the mean of the first 22 data points obtained at membrane potential = $HP - I_{leak} \times R_s$. In the next step, the leak current ($(TP - I_m \times R_s)/R_{leak}$) was subtracted from the membrane current, and the membrane conductance for potassium ions (G_K) was calculated for each data point using ($TP - I_m \times R_s - E_{rev}$) driving force. Thus, the resulting G_K is corrected for both linear leak and voltage error caused by series resistance, and was used to reconstruct the current trace at TP. The Marquardt-Levenberg algorithm was used to fit the appropriate equations to the decaying part of the current traces. The fits were evaluated by the sum of squared differences between the measured and calculated data points ($SSE = \Sigma(y - \hat{y})^2$). Activation time constants were determined by fitting current traces (uncorrected) to the function $A \cdot (1 - e^{-t/\tau})^4 + B$, using the pClamp software (Axon Instruments, Foster City, CA). Box plots were used to represent the central tendency of the measured parameters. The box and the bars indicate 25–75 and 10–90 percentile of the data, respectively, and the circles represent data <10 and >90 percentile.

Recombinant DNA techniques

Standard methods of plasmid DNA preparation, restriction enzyme analysis, agarose gel electrophoresis, and bacterial transformations were used (Deutsch and Chen, 1993; Tu et al., 1995). The mutation of alanine to valine at position 413 was made using the PLATER-1 mutagenesis system (Promega, Madison, WI), and was verified by DNA sequence analysis (Sequenase Version 2.0 DNA sequencing kit, USB, Inc., Cleveland, OH). Wild-type and mutant Kv1.3 inserts (1.8 kb) were cloned into a pRc-based plasmid containing a CMV eukaryotic promoter sequence (5.4 kb), yielding the pRc/CMV/WT and pRc/CMV/A413V plasmids (Deutsch and Chen, 1993). The Ccd4neo plasmid is a pUC-based plasmid (5.0 kb) with a CMV promoter, and contains the gene for human CD4 (1.7 kb, gift from Ray Sweet, SmithKline Beecham).

Construction of double gene plasmid containing mutant Kv1.3 (A413V) and human CD20

To clone pRc/CMV/A413V plus human CD20, a *Bgl*II blunt-ended/*Xho*I blunt-ended digested fragment was isolated from pRc/CMV/Kv1.3(A413V) and ligated into *Hin*dIII partially digested blunt-ended/*Xba*I blunt-ended digested pRc/CMV-neo-*Bam*/CD20. The final double gene plasmid is 8.7 kb.

RESULTS AND DISCUSSION

To investigate the molecular basis for C-type inactivation we have selected a point mutant of Kv1.3, which itself produces K^+ current with markedly faster macroscopic inactivation kinetics than the wild-type current. Based on the work of Hoshi et al. (1991), who reported that an A463V mutation in the S6 segment of *Shaker* B accelerated the rate of C-type inactivation, we mutated the equivalent alanine in Kv1.3 to a valine (A413V). We have expressed separately wild-type (WT) and A413V mutant subunits of Kv1.3 in mouse cytotoxic T cells, CTLL-2, which lack endogenous K^+ current (Deutsch and Chen, 1993). The corresponding current traces in response to a depolarization to +50 mV are shown in Fig. 1. The properties of wild-type voltage-gated K^+ currents produced by heterologously expressed channels in CTLL-2 cells and by endogenously expressed channels in human T lymphocytes are virtually identical (Deutsch and Chen, 1993; Tu et al., 1995). The medians of the measured inactivation time constants for WT and A413V homotetrameric currents are 204 and 4 ms, respectively. To establish whether one or more subunits is sufficient to determine C-type inactivation, we co-transfected CTLL-2 with both WT and A413V in various ratios, using plasmids that also encode for a surface marker (CD4 or CD20). Co-transfection of surface markers allowed us to select positive transfectants for electrophysiological recording (Deutsch and Chen, 1993). The resultant currents manifested inactivation kinetics intermediate between those for WT and A413V (see below). The current decay could always be approximated by a single exponential function to give inactivation time constants ranging from 11 to 147 ms (nine cells; see Table 1).

We examined three models that could account for the observed inactivation kinetics. In model I, a mixture of homotetramers yields the observed intermediate kinetics. In model II, each subunit of a homo- and heterotetrameric channel acts independently, while in model III, all four subunits participate cooperatively to produce the apparent inactivation kinetics.

Model I predicts that WT and A413V subunits do not form heterotetrameric channels. If this were true, then the decay of the current should be well-described by a double-

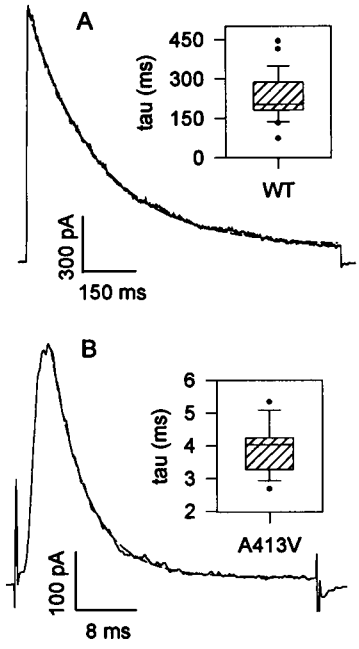

FIGURE 1 Whole cell K^+ currents in CTLL-2 cells transfected with WT or A413V Kv1.3. (*A* and *B*) Current was elicited by a voltage step from the holding potential to +50 mV for 900 ms for cells transfected with Kv1.3 WT (*A*) or for 40 ms for A413V (*B*). The fit of a single exponential decay function to each current trace (- - - - -) resulted in τ = 196 ms and τ = 4.7 ms, respectively. Note difference in time scale. The insets show the box plot of inactivation time constants for cells expressing WT (n = 24, median = 203.9 ms) or A413V homotetramer channels (n = 10, median = 4.03 ms). Holding potential, cell capacitance, and series resistance were −120 mV, 6.6 pF, and 3.8 MΩ (corrected) for WT (*A*); and −130 mV, 6.5 pF, and 12.8 MΩ for A413V (*B*), respectively.

exponential function, in which each exponential term contains the characteristic inactivation time constants for pure WT and A413V current, and is weighted by the fraction of the two homotetrameric channels. Since the WT/A413V mixtures never produced currents with clearly biphasic relaxations, heteromultimers must be present, eliminating model I as an explanation for the observed kinetics. We verify this conclusion by statistical analysis (below).

Three cases (1–3) of independence may be considered for model II to produce the observed kinetics. In case 1, by analogy with N-type inactivation (MacKinnon et al., 1993), any one and only one of four subunits causes inactivation, and recovery from inactivation depends on the return of this subunit to its non-inactivated conformation. In case 2, the channel is inactivated only if each of four subunits is in an inactivated conformation. This mechanism is analogous to K^+-channel activation models and predicts a delay in the onset of inactivation of the current. In case 3, the channel is inactivated if any of the four subunits is in an inactivated conformation. This differs from case 1 in that the inactivation by a single subunit does not prevent other subunits from adopting inactivated conformations. This mechanism predicts a delay in recovery from inactivation. Case 1 is a simple two-state, one-step process for both entry into and exit from the inactivated state, whereas cases 2 and 3 contain multiple steps to enter (case 2) or to exit (case 3) the inactivated state. We have eliminated case 2 for WT Kv1.3 because of the absence of a delay in the onset of inactivation (Fig. 2). Since the measured activation and inactivation time constants for WT currents in CTLL-2 at +50 mV are 1.67 ± 0.18 ms (SEM, n = 7) and 233.8 ± 18.6 ms (SEM, n = 24), respectively, all the channels have opened before inactivation occurs (see measured first latencies in Lee et al., 1992). Thus, a significant lag in onset of inactivation could have been detected. Similarly, no delay in C-type inactivation has been observed for mutant *Shaker* B channels (D. Sigg, S-A. Seoh, and D. Papazian, personal communication). We evaluated case 3 by fitting the kinetics for recovery from inactivation for WT Kv1.3 to either a single-exponential relaxation or a fourth-power sigmoidal function, i.e., a delay (Fig. 2). Because these fits to the recovery data failed to discriminate clearly between these two functions, we tested case 3 by statistical analysis of heteromultimeric current inactivation kinetics at a depolarized voltage (below). Therefore, only cases 1 and 3 have been considered in our evaluation of model II (see below).

Theory and statistical analysis

Kv1.3 channels are closed at very negative voltages. However, at a strongly depolarized membrane voltage only a negligible fraction of channels reside in a closed state (Lee et al., 1992). Therefore, a simple reaction scheme to describe the decay of the current uses only an open and an inactivated state and can be written as:

$$O \underset{k_{r,m}}{\overset{k_{i,m}}{\rightleftharpoons}} I \qquad (1)$$

where $k_{i,m}$ and $k_{r,m}$ are the rate constants for inactivation and recovery from inactivation, respectively, for a channel containing m mutant (A413V) subunits. A channel that has been opened by depolarization will be inactivated at steady-state with a probability of $k_{i,m}/(k_{r,m} + k_{i,m})$, whereas the probability that it will not be inactivated is $k_{r,m}/(k_{r,m} + k_{i,m})$. The latter probability is equal to the ratio (R) of measured steady-state current to peak current. To determine R we restricted the data to (1) those cells with input resistance >2 GΩ to obviate error introduced by leak compensation and (2) selected current traces that contained data values at pulse durations >4 times the inactivation time constant to ensure that the steady state had been reached. As shown in Fig. 3 for channels formed from only WT, from only A413V, or from a mixture of WT/A413V subunits, there was no significant difference between the median value of R for the three groups, as determined by Kruskal-Wallis one way ANOVA on ranks (p = 0.76). For all of the data (i.e., WT, A413V, and the heteromultimers) peak current exhibits a strong linear dependence on steady-state current (data not shown), as determined by nonparametric Spearman analysis; the correlation coefficient is 0.78 ($p < 10^{-11}$, n = 75). Therefore the probability R is independent of subunit com-

TABLE 1 The cooperative model gives an excellent fit over a wide range of macroscopic current inactivation rates

Cell	τ (ms)	Model I		Model II case 1		Model II case 3		Model III	
		f	SSE	P	SSE	P	SSE	P	SSE
A	10.7	0.88	5.48	0.43	0.25	0.73	3.23	0.79	0.34
B	16.1	0.87	3.57	0.37	0.23	0.75	2.34	0.74	0.21
C	26.2	0.78	2.17	0.27	0.49	0.66	1.92	0.56	0.09
D	45.8	0.7	2.76	0.25	0.74	0.50	2.22	0.49	0.09
E	58.1	0.56	7.37	0.18	1.86	0.27	4.1	0.36	0.07
F	87.6	0.52	1.4	0.16	0.4	0.32	1.13	0.32	0.19
G	103.6	0.39	1.65	0.11	0.66	0.12	0.65	0.23	0.1
H	139	0.25	0.68	0.07	0.42	0.11	0.51	0.14	0.11
I	147	0.21	0.8	0.05	0.31	0.01	0.13	0.12	0.08

This table shows the parameters P (the estimated fraction of mutant subunits) or f (the estimated fraction of A413V homotetramers) and the sum of squared errors for fits of models I–III to selected current traces from cells A-I. Apparent time constants, τ, were estimated using a single-exponential function.

position. We assume that the values of peak current used to calculate R values are accurately measured from the observed current maxima in the raw data traces. This assumption holds for WT and heteromultimers. In the latter case, the fastest time constant for inactivation at +50 mV is 10.7 ms (Table 1), which is five times the activation time constant. In the case of WT currents, the activation and inactivation time constants differ by two orders of magnitude. Our assumption, however, may not hold for A413V currents because the activation and inactivation time constants at +50 mV are 1.43 ± 0.08 ms (SEM, n = 11) and 3.94 ± 0.25 ms (SEM, n = 10), respectively. It is therefore not possible to get an unambiguous value for peak activation in A413V mutants. Extrapolation of inactivation kinetics to zero time is not a valid solution because this assumes that activation and C-type inactivation are independent, which may not be true. The only consequence of a possible error in A413V peak current is that R for A413V mutant may be overestimated. However, this will not affect the outcome of the statistical analyses, which were applied only to currents produced by mixtures of WT and mutant subunits (see below).

Assuming a binomial distribution for the formation of heteromultimeric channels from four subunits (MacKinnon et al., 1993), the normalized current can be described by

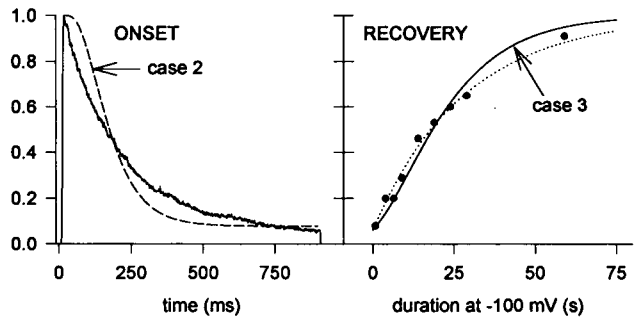

FIGURE 2 Model for delayed onset and recovery from inactivation for Kv1.3 WT. (*Left*) Delay is shown in the onset of inactivation of the macroscopic current (- - - - -), predicted by model II, case 2. The current trace is the same as in Fig. 1 *A*. The decaying part of the normalized current was fit with the equation $I(t)/I_{peak} = 1\text{-}(U\cdot(1 - e^{-t/\tau'}))^4$, assuming that all the channel subunits are in the non-inactivated conformation at the peak of the current, i.e., $t = 0$. The value of $U = 0.98$ was calculated from the ratio of steady-state current to peak current, R, according to $U = (1 - R)^{1/4}$, and corresponds to the probability of a subunit being in an inactivated conformation at steady state. The resulting $\tau' = 81.2$ ms is the estimated time constant for the relaxation of the subunit transitions. (*Right*) Delay of recovery from inactivation is shown assuming model II, case 3 (——). The holding potential was −100 mV. A prepulse (1 s) to +50 mV was followed after the indicated times at −100 mV by a test pulse to +50 mV for 1 s. (●) Ratio of the peak currents during the test pulse to peak currents during the prepulse (I_2/I_1). (·····) An exponential function, $I_2/I_1 = A_r\cdot(1 - e^{-t/\tau}) + C_r$ with $A_r + C_r = 1$, fit to the data points (τ = 28.2 s). Model II case 3 was modeled by the equation, $I_2/I_1 = (1 + (R' - 1)\cdot e^{-t/\tau'})^4$, in which the probability of a subunit being in the non-inactivated conformation varies from an initial value of R' to 1 with a time constant τ'. Fitting this equation to the data gives $\tau' = 16.1$ s. $R' = R^{1/4}$, with $R = 0.0625$ calculated from the prepulse current as described above.

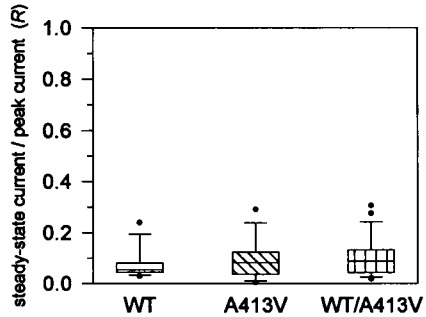

FIGURE 3 The ratio of steady-state to peak current for CTLL-2 expressing WT or A413V homotetramers or a mixture of WT/A413V hetero- and homotetramers. The ratio (R) of the steady-state current to the peak current was determined from current traces evoked by depolarizations to +50 mV form the holding potential. The current was corrected for ohmic leak and voltage error caused by series resistance, as described in Materials and Methods. The median of R (R_{50}, *horizontal line*) was 0.055 and 0.082 for cells expressing WT (n = 10), and A413V (n = 9) homotetrameric channels, respectively, and 0.088 for cells expressing a mixture of WT/A413V hetero- and homotetrameric K^+ channels (n = 21). There was no significant difference between the median value of R for the three groups (Kruskal-Wallis one-way ANOVA on ranks, p = 0.76).

the following equation:

$$\frac{I(t)}{I_{peak}} = \sum_{m=0}^{4} \frac{4!}{m!\,(4-m)!} P^{m}(1-P)^{4-m} \times ((1-R)e^{-t(k_{i,m}+k_{r,m})} + R) \quad (2)$$

where P is the estimated fraction of mutant subunits in the cell membrane, and m indicates the number of mutant (A413V) subunits in a given channel. The WT homotetramer is represented by $m = 0$, whereas $m = 4$ describes the homomultimeric A413V channel. In Eq. 2, the only term that depends on the subunit composition of the channels is the sum of the rate constants for inactivation and recovery from inactivation ($k_{i,m} + k_{r,m}$). Examples of heteromultimeric currents are shown in Fig. 4 along with calculated currents derived, as described below, for models I–III.

In model I the normalized current is given by the weighted sum of two exponential terms:

$$\frac{I(t)}{I_{peak}} = f(1-R)e^{-t/\tau_4} + (1-f)(1-R)e^{-t/\tau_0} + R \quad (3)$$

where f is the fraction of A413V homotetramers, R is the ratio of steady-state-to-peak current for a given trace, and $\tau_4 = 4$ ms and $\tau_0 = 204$ ms are the medians of macroscopic inactivation time constants for A413V and WT currents, respectively. In fitting data to this equation, f was the only free parameter. Because of the clear separation of the time constants the theoretical curves have biphasic character and deviate substantially from the experimental current traces (Fig. 4 and Table 1).

In model II case 1, each subunit acts independently and entry into and exit from the inactivated state of the channel is associated with a two-state transition of any one and only one of the four subunits. Each subunit inactivates with a rate constant k'_i and recovers from inactivation with a rate constant k'_r. For a homotetrameric channel the rate of inactivation, k_i, is $4\times k'_i$ and the rate of recovery, k_r, is k'_r (MacKinnon et al., 1993; Gomez-Lagunas and Armstrong, 1995). Therefore the corresponding rate constants for each subunit can be calculated from the medians of R and inactivation time constants ($\tau_m = (k_{i,m} + k_{r,m})^{-1}$) for WT ($m = 0$) and A413V ($m = 4$) homotetrameric currents. The probability that a heteromultimeric channel will be inactivated by an A413V subunit equals $m \cdot k'_{i,A413V}/(m \cdot k'_{i,A413V} + (4-m) \cdot k'_{i,WT})$, where m is the number of A413V subunits in the channel. In the limiting case in which

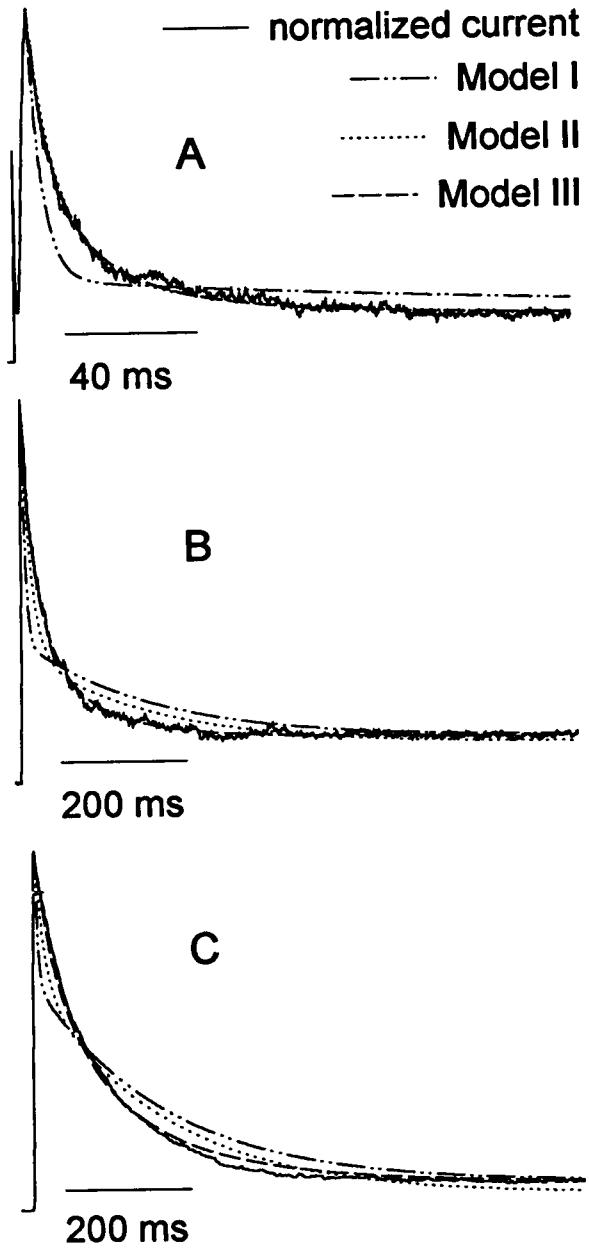

FIGURE 4 Whole cell currents from CTLL-2 expressing mixtures of WT/A413V homo- and heterotetramers. In *A–C* three different cells were co-transfected with a double gene plasmid containing Kv1.3 A413V and human CD20 gene inserts along with a plasmid containing the WT channel gene, and currents were recorded during a step from +50 mV from a holding potential of −120 mV as described in Materials and Methods and Matteson and Deutsch (1984). Pulse durations were 180, 900, and 900 ms for *A*, *B*, and *C*, respectively. The resultant currents were normalized to their respective peak values, and the decaying portions were fit with models I–III. In all cases (*A–C*), model I (— ·· — ··) gives a very poor fit (see Table 1). (*A*) This cell is the same as cell B, (Table 1) and has a capacitance of 5 pF, series resistance of 7.7 MΩ, peak current of 530 pA and fast inactivation kinetics. The cooperative model (model III, - - - - -) gives $P = 0.74$ (sum of squared errors, SSE = 0.21; ratio of steady-state current to peak current, $R = 0.1$). The independent model (model II, case 1, ····) gives $P = 0.37$, $k_{r,0} = 4.63 \cdot 10^{-8}$ s^{-1}, $k_{r,m} = 4.28$ s^{-1} (SSE = 0.23). (*B*) This cell is the same as cell D, (Table 1), and has a capacitance of 14 pF, series resistance of 5.9 MΩ, peak current of 407 pA, and intermediate inactivation kinetics. Model III gives an excellent fit with $P = 0.49$ (SSE = 0.09, $R = 0.085$), while model II gives a poor fit with $P = 0.25$, $k_{r,0} = 1.01$ s^{-1}, $k_{r,m} = 4.23 \cdot 10^{-7}$ s^{-1} (SSE = 0.74). (*C*) This cell is the same as cell G (Table 1) and has a capacitance of 4.9 pF, series resistance of 6.2 MΩ, peak current of 1250 pA, and slow inactivation kinetics. Model III gives an excellent fit with $P = 0.23$ (SSE = 0.10, $R = 0.035$), while model II gives a poor fit with $P = 0.11$, $k_{r,0} = 2.47 \cdot 10^{-8}$ s^{-1}, $k_{r,m} = 1.27 \cdot 10^{-6}$ s^{-1} (*SSE* = 0.66).

three of the four subunits are wild-type ($m = 1$), the probability that the channel will be inactivated by a mutant subunit is 0.94. This probability increases to 1.0 as the number of A413V subunits increases to four, confirming that the number of mutant subunits will determine the rate of inactivation of the heterotetramers. Thus,

$$k_{i,m} = \frac{m}{4} k_{i,4} \tag{4}$$

The rate of recovery from inactivation depends only on the return of this single A413V subunit to the non-inactivated state. Therefore, for $m = 1$–4, $k_{r,m}$ is constant and equals $k_{r,4}$. This model can be eliminated for two reasons. First, the fraction of steady-state current, R, which equals $k_{r,m}/(k_{i,m} + k_{r,m})$, will decrease with the number of mutant subunits in this model, in contradiction to our data (Fig. 3). Second, according to this model the expected time constants for heteromultimeric currents cannot exceed four times that for the mutant homomultimer. This follows from the fact that the maximum ratio of heteromultimer-to-homomultimer time constants is $(k_{i,4} + k_{r,4})/(k_{i,1} + k_{r,4}) \leq 4$, in contradiction to our data (Fig. 4. and Table 1). The normalized current was fit for case 1, model II, using Eq. 2. From the medians of inactivation time constants for A413V and WT current, and Eq. 4, we expressed R as a function of $k_{r,4}$ and $k_{r,0}$:

$$R_m = \frac{k_{r,4}}{\frac{m}{4\tau_4} + k_{r,4}\left(1 - \frac{m}{4}\right)} \quad \text{for} \quad m > 0,$$

and

$$R_0 = k_{r,0}\tau_0 \quad \text{for} \quad m = 0 \tag{5}$$

and allowed these two rate constants, in addition to P, to be free parameters. Although the resulting equation has two more degrees of freedom, compared with the fitting equation for model III (see below), the fits for the current traces having intermediate or slow inactivation kinetics are poor (Fig. 4, Table 1).

In model II case 3, a channel is open only if all four subunits of the channel are in the conducting conformation, but all subunits can adopt the inactivated conformation. Therefore, the open probability of a channel as a function of time will depend on the product of the relaxation of subunit transitions. Eq. 2 was modified accordingly to describe the heteromultimeric currents:

$$\frac{I(t)}{I_{peak}} = \sum_{m=0}^{4} \frac{4!}{m!\,(4-m)!} P^m (1-P)^{4-m} \times [(1-R')e^{-t/\tau'_{A413V}} + R']^m [(1-R')e^{-t/\tau'_{WT}} + R']^{4-m} \tag{6}$$

R' represents the probability of a subunit being in the non-inactivated state at steady state, and τ'_{A413V} and τ'_{WT} are the relaxation time constants for a single mutant and WT subunit, respectively. Since R, the measured ratio of steady-state current to peak current, is independent of the subunit composition of the channels, R' for an A413V subunit is equal to R' for a WT subunit and can be calculated for a given trace according to $R' = R^{1/4}$. The median values of $\tau_4' = 7.83$ ms ($n = 7$) and of $\tau_0' = 306.3$ ms ($n = 11$) were obtained by fitting Eq. 6 to A413V and WT homotetrameric currents, respectively ($P = 1$ and $m = 4$ for A413V currents, and $P = 0$ and $m = 0$ for WT currents). Eq. 6 has only one free parameter, P. The fits to the heterotetrameric current traces were generally very poor, especially when the inactivation rate of the current was fast (Table 1).

In model III, cooperativity is expressed in the rate constants for inactivation ($k_{i,m}$) and recovery ($k_{r,m}$). Since R is constant (Fig. 3), $k_{i,m}/k_{r,m}$ is a constant for any subunit composition. Therefore, we may use a single cooperativity factor, F, for both rate constants, according to the following equation:

$$k_{i,m} + k_{r,m} = (\nu_i + \nu_r)F^m = \frac{1}{\tau_m} \tag{7}$$

where $\nu_i + \nu_r$ is the sum of the respective rate constants when $m = 0$ (only homotetrameric WT channels). Substituting the median homotetrameric τ_0 (204 ms) and τ_4 (4 ms) into Eq. 7 for $m = 0$ and $m = 4$, respectively, we calculated $F = 2.67$. Thereafter τ_m was determined for each value of m (Eq. 7), and used in Eq. 2 to fit individual current traces. Since R was measured for each current trace, the only free parameter in Eq. 2 is P, the estimated fraction of A413V subunits in the membrane. This parameter cannot be predicted precisely because of the stochastic nature of the transfection; however, there was a correlation of P with ratios of WT/A413V DNA used in the transfection. An increased frequency of cells manifesting longer single-

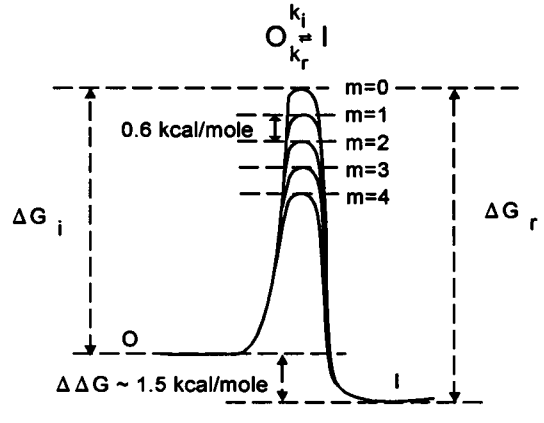

FIGURE 5 Energy state diagram of the transitions between open and inactivated states of the channels based on the cooperative model. The transition from the open (O) to the inactivated (I) state occurs with a rate constant k_i for the energy barrierΔG_i. The recovery from the inactivated state (I → O) occurs with a rate constant k_r for the energy barrier ΔG_r. The difference in free energy between the open and inactivated states of the channel is denoted by $\Delta\Delta G$. The height of the energy barrier depends on the number of mutant subunits (m) in the tetrameric channel (see text). The energy levels are not drawn to scale.

exponential time constants was observed when a higher molar ratio of WT/A413V DNA was used. Although Eq. 2 is highly constrained (i.e., only one free parameter), it gives excellent fits for a variety of current traces with markedly different inactivation rates (Fig. 4, Table 1).

Fig. 4 shows the measured current traces for three of nine cells (*B*, *D*, and *G* in Table 1), along with the calculated currents derived from best fits for each of the three models. We show only case 1 for model II because in general this case gave a better fit than case 3 across the entire range of data (Table 1). These three cells represent a range of observed single-exponential inactivation time constants: 16.1, 45.8, and 103.6 ms, respectively, each well fit by the cooperative model to give calculated predominant channel types containing 3, 2, and 1 A413V subunits, respectively. As shown in Table 1, the independent model, for both cases 1 and 3, does not fit the data as well as the cooperative model, despite two additional degrees of freedom included for the fits for case 1. Our results show that WT and A413V subunits form heteromultimeric channels since the model based on a mixture of homotetramers only (model I) fails to fit the data for any cell.

Based on the cooperative model, we have constructed an energy state diagram (Fig. 5) of the transitions between open (O) and inactivated (I) states of Kv1.3 at +50 mV. In this description, the difference in free energy between the open and inactivated states of the channel is shown as $\Delta\Delta G$ and is equal to $-RT \ln k_{r,m}/k_{i,m}$. To compute $\Delta\Delta G$, we used $k_{i,4} = 227.8\ s^{-1}$ and $k_{r,4} = 20.3\ s^{-1}$ for A413V and $k_{i,0} = 4.63\ s^{-1}$ and $k_{r,0} = 0.27\ s^{-1}$ for WT homotetramers. These rate constants were calculated from the respective medians of inactivation time constants and medians of *R* (Figs. 1, *A* and *B*, and 3) for A413V and WT homotetramers. The value of $\Delta\Delta G$ is ~1.5 kcal/mol and is invariant with subunit composition because the ratio of $k_{r,m}/k_{i,m}$ is the same for all channel types. If k_i and k_r increase as the number of A413V subunits increases in the tetramer, but the ratio of these rate constants remains unchanged, then only the transition state energy is altered by additional A413V subunits. The relationship between k_i (or k_r) and ΔG_i (or ΔG_r) is given by the Eyring equation,

$$k_i = \frac{kT}{h} e^{-\Delta G_i/RT} = \frac{kT}{h} e^{-A_i/RT} e^{-B_i/RT},$$
$$k_r = \frac{kT}{h} e^{-\Delta G_r/RT} = \frac{kT}{h} e^{-A_r/RT} e^{-B_r/RT} \quad (8)$$

We define ΔG as the sum of two terms: *A*, the free energy associated with inactivation transitions of the WT homotetramer channel, and *B*, the additional energy contributed by A413V subunits to the O $\rightleftharpoons$ I transitions. Comparing Eq. 8 for k_i and k_r with Eq. 7 we assign ν_i (or ν_r) to the first exponential term containing A_i (or A_r), respectively, and F^m to the second exponential term containing B_i (or B_r). Thus $B_i = B_r = -RTm \ln F$. Each mutant subunit contributes equally to the activation free energy for transitions between open and inactivated states, with an A413V subunit decreasing ΔG_i (and ΔG_r) by ~0.6 kcal/mol.

Our results are consistent with a cooperative model for Kv1.3 C-type inactivation in situ, similar to a preliminary report for *Shaker* channels expressed in oocytes (Ogielska et al., 1994). A physical mechanism by which C-type inactivation occurs has not been proven, although one plausible suggestion is that the outer mouth of the channel constricts, thereby decreasing the inter-subunit distance across this outer vestibule (Yellen et al., 1994). Another possible mechanism is that subunits each participate equally in a cooperative process to create a binding site for an "inactivation particle," which presumably would reside near the outer mouth of the channel. Cooperativity has been demonstrated for the creation of an external TEA binding site in a mutant *Shaker* channel. Heginbotham and MacKinnon (1992) and Kavanaugh et al. (1992) showed that external TEA interacts simultaneously with several subunits. Each of the four subunits contribute approximately equally to the formation of the external TEA binding site (Heginbotham and MacKinnon, 1992; Hurst et al., 1992). However, it is less likely that the mechanism underlying cooperative C-type inactivation is cooperative formation of a binding site, since the putative extracellular loops between transmembrane segments in Kv1.3 are too small to accommodate such a tethered inactivation particle.

It is C-type inactivation that is solely responsible for inactivation in Kv1.3, the predominant channel found in T lymphocytes. Inactivation limits the amount of available K^+ current, which in the case of human T cells is important for cellular functions such as volume regulation (Deutsch and Chen, 1993) and membrane potential-dependent interleukin-2 production (Freedman et al., 1992). Thus, understanding the mechanism of C-type inactivation may be critical to our comprehension of T-cell physiology and immune responsiveness.

Note added in proof: CTLL-2 transfected with Kv1.3WT-A413V tandem dimer constructs produced currents at +50 mV that displayed single exponential decays with the predicted decrease in the inactivation time constant compared to currents expressed from tandem dimers of Kv1.3 WT-WT. These results are consistent with the cooperative model, and similar to results obtained with *Shaker* tandem dimers expressed in oocytes (Ogielska et al., 1994).

We thank Dr. Richard Horn for his critical reading of the manuscript, help with the computer programming, and suggestions for the mathematical analysis; Daniel Levy for computer programming; and Daniel Sigg for helpful discussions. This work was supported by National Institutes of Health grant GM 41476 and GM 52302, a University of Pennsylvania Research Foundation grant, and grant FO5 TWO 5079 from the Fogarty International Center, National Institutes of Health. The contents of the publication are solely the responsibility of the authors and do not necessarily represent the official views of the Fogarty International Center, National Institutes of Health.

REFERENCES

Choi, K. L., R. W. Aldrich, and G. Yellen. 1991. Tetraethylammonium blockade distinguishes two inactivation mechanisms in voltage-activated K^+ channels. *Proc. Natl. Acad. Sci. USA.* 88:5092–5095.

Demo, S. D., and G. Yellen. 1991. The inactivation gate of the *Shaker* K^+ channel behaves like an open-channel blocker. *Neuron.* 7:743–753.

Deutsch, C., and L-Q. Chen. 1993. Heterologous expression of specific K^+ channels in T lymphocytes: functional consequences for volume regulation. *Proc. Natl. Acad. Sci. USA.* 90:10036–10040.

Freedman, B. D., M. Price, and C. Deutsch. 1992. Evidence for voltage modulation of IL-2 production by human blood lymphocytes. *J. Immunol.* 149:3784–3794.

Gomez-Lagunas, F., and C. Armstrong. 1995. Inactivation in *Shaker* B K^+ channels: a test for the number of inactivating particles on each channel. *Biophys. J.* 68:89–95.

Grissmer, S., and M. Cahalan. 1989. TEA prevents inactivation while blocking open K^+ channels in human T lymphocytes. *Biophys. J.* 55:203–206.

Heginbotham, L., and R. MacKinnon. 1992. The aromatic binding site for tetraethylammonium ion on potassium channels. *Neuron.* 8:483–491.

Hoshi, T., W. N. Zagotta, and R. W. Aldrich. 1991. Two types of inactivation in *Shaker* K^+ channels: effects of alterations in the carboxy-terminal region. *Neuron.* 7:547–556.

Hurst, R. S., M. P. Kavanaugh, J. Yakel, J. P. Adelman, and R. A. North. 1992. Cooperative interactions among subunits of a voltage-dependent potassium channel. *J. Biol. Chem.* 267:23742–23745.

Kavanaugh, M. P., R. S. Hurst, J. Yakel, M. D. Varnum, J. P. Adelman, and R. A. North. 1992. Multiple subunits of a voltage-dependent potassium channel contribute to the binding site for tetraethylammonium. *Neuron.* 8:493–497.

Lee, S. C., D. I. Levy, and C. Deutsch. 1992. Diverse K^+ channels in primary human T lymphocytes. *J. Gen. Physiol.* 99:771–793.

Levy, D. I., G. Panyi, Z. Sheng, L.-W. Tu, and C. Deutsch. 1995. C-type inactivation determined by multiple subunits. *Biophys. J.* 68:A33 (Abstr.).

López-Barneo, J., T. Hoshi, S. H. Heinemann, and R. W. Aldrich. 1993. Effects of external cations and mutations in the pore region on C-type inactivation of *Shaker* potassium channels. *Recept. Channels.* 1:61–71.

MacKinnon, R., R. W. Aldrich, and A. W. Lee. 1993. Functional stoichiometry of *Shaker* potassium channel inactivation. *Science.* 262:757–759.

Matteson, D. R., and C. Deutsch. 1984. K^+ channels in T lymphocytes: a patch clamp study using monoclonal antibody adhesion. *Nature.* 307: 468–471.

Ogielska, E. M., W. N. Zagotta, and R. W. Aldrich. 1994. The stoichiometry of C-type inactivation. *Biophys. J.* 66:A282 (Abstr.).

Tu, L.-W., V. Santarelli, and C. Deutsch. 1995. Truncated K^+ channel DNA sequences specifically suppress lymphocyte K^+ channel gene expression. *Biophys. J.* 68:147–156.

Yellen, G., D. Sodickson, T. Chen, and M. E. Jurman. 1994. An engineered cysteine in the external mouth of a K^+ channel allows inactivation to be modulated by metal binding. *Biophys. J.* 66:1068–1075.

Zagotta, W. N., T. Hoshi, and R. W. Aldrich. 1990. Restoration of inactivation in mutants of *Shaker* potassium channels by a peptide derived from ShB. *Science.* 250:568–571.